



 Cite this: *RSC Adv.*, 2024, 14, 24781

Design, synthesis, and antiproliferative screening of new quinoline derivatives bearing a *cis*-vinyl triamide motif as apoptosis activators and EGFR-TK inhibitors†

 Hany M. Abd El-Lateef,^{*ab} Ahmed Gaafar Ahmed Gaafar,^c Arwa Sultan Alqahtani,^d Aamal A. Al-Mutairi,^d Dalal Sulaiman Alshaya,^e Fahmy Gad Elsaid,^f Eman Fayad^g and N. A. Farouk ^{*h}

In this work, a congeneric set of quinoline-tethered *cis*-vinyl triamide hybrids was prepared and evaluated as EGFR tyrosine kinase inhibitors for the management of breast cancer. All of the prepared hybrids were evaluated for their antiproliferative effect against the breast MCF-7 cell line. Among the tested hybrids, compound **6f** displayed the most potent antiproliferative activity with an IC₅₀ value of 1.87 μM compared to STU (IC₅₀ = 13.71 μM) as the standard reference. The most promising hybrid, **6f**, was found to induce cellular cycle arrest at the G1 phase. Furthermore, the molecular mechanism of this hybrid revealed its ability to induce cellular apoptosis *via* the mitochondrial-dependent apoptotic pathway. Compound **6f** decreased MCF-7 cells' MMP compared to the controls (percentage change value of 57.93%). Further investigation of the selective compound **6f** showed that it can inhibit EGFR tyrosine kinase.

 Received 8th July 2024
 Accepted 29th July 2024

DOI: 10.1039/d4ra04915b

rsc.li/rsc-advances

1. Introduction

Cancer remains the leading cause of death in the world, second only to heart disease.^{1,2} Cancer itself is a dynamic, complex cellular network of uncontrolled growth.³ Of all cancer subtypes, breast cancer is one of the most deadly, and also consistently beckons the largest number of new diagnoses among women.^{4,5} Clearly, there is a serious unmet demand for therapies targeting this cancer subtype.^{6,7} Effective chemotherapeutic treatments with minimal side effects are urgently needed, particularly in the face of the increasing prevalence of drug-resistant tumors.⁸

Therapies based on targeted biological target are intended to be less toxic than conventional chemotherapy.^{9,10}

The epidermal growth factor receptor (EGFR), being one of the most prominent protein kinases, plays a vital role in a series of cellular processes during the life cycle of the cell, such as the regulation of cell migration and cell division.^{11,12} Multiple prospective clinical trials were initiated to test the efficacy of EGFR-targeted therapy *versus* standard chemotherapy.¹³ Clinical trials revealed definite evidence of the superiority of EGFR tyrosine kinase inhibitors over standard chemotherapeutic regimens.¹⁴ Targeted inhibitors of EGFR signalling inhibited ligand-induced EGFR auto-phosphorylation and attenuated downstream signalling responsible for proliferation and survival of the cells.^{15,16} The inhibition of EGFR signalling leads, in most cases, to cell cycle arrest and/or drug-induced apoptosis.^{17,18} Therefore, EGFR has been regarded as an attractive target for the establishment of chemotherapeutic drugs for many cancers.¹⁹ Accordingly, the discovery of new EGFR has attracted a great deal of attention in recent years.²⁰

Quinolines are a distinct class of fused bicyclic hetero-aromatic core compounds that have developed into a very popular research topic.^{21–23} Several quinoline-based compounds are known to have chemical, biological and therapeutic applications.^{24,25} They were found to exhibit anticancer, antiviral and antimicrobial effects.^{26–28} The quinoline nucleus is also an integral component of several anticancer drugs, which have revolutionized the therapy of cancer disease.^{29–31} The anti-cancer activity seems to be due to a variety of mechanisms

^aDepartment of Chemistry, College of Science, King Faisal University, Al-Ahsa 31982, Saudi Arabia. E-mail: hmahmed@kfu.edu.sa

^bDepartment of Chemistry, Faculty of Science, Sohag University, Sohag 82524, Egypt

^cDepartment of Pharmacology and Toxicology, Faculty of Pharmacy, Port Said University, Port Said, Egypt

^dDepartment of Chemistry, College of Science, Imam Mohammad Ibn Saud Islamic University(IMSUI), P.O. Box 90950, Riyadh 11623, Saudi Arabia

^eDepartment of Biology, College of Science, Princess Nourah bint Abdulrahman University, P.O. Box 84428, Riyadh 11671, Saudi Arabia

^fDepartment of Biology, College of Science, King Khalid University, PO Box 960, Abha, 61421, Asir, Saudi Arabia

^gDepartment of Biotechnology, College of Sciences, Taif University, P.O. Box 11099, Taif 21944, Saudi Arabia

^hDepartment of Chemistry, Faculty of Science, Port Said University, Port Said, Egypt. E-mail: nesmafarouk566@gmail.com

† Electronic supplementary information (ESI) available. See DOI: <https://doi.org/10.1039/d4ra04915b>



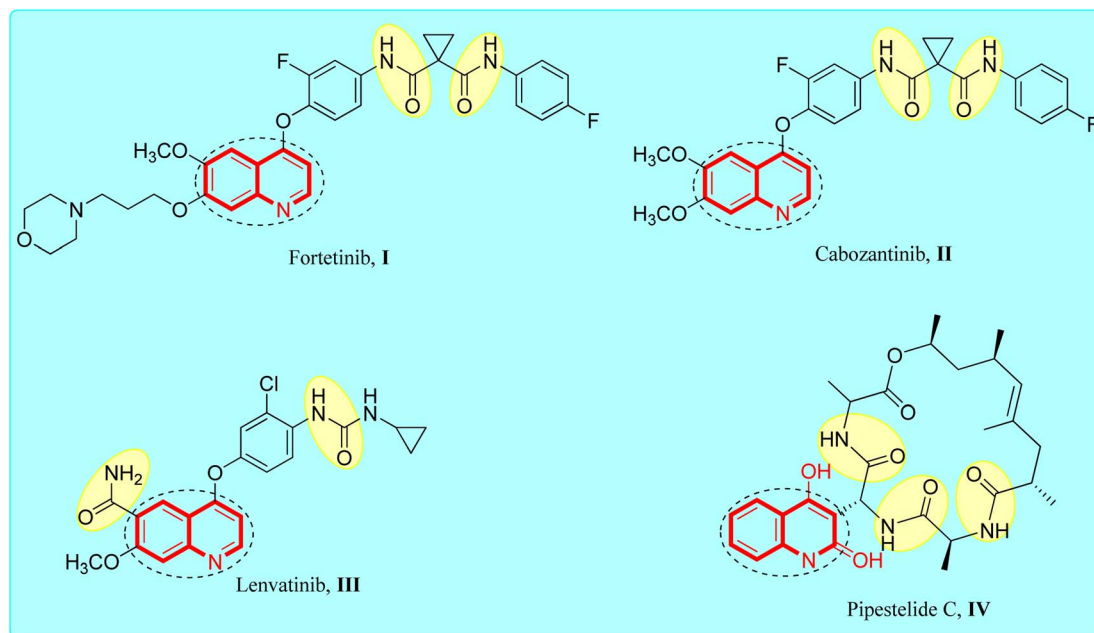


Fig. 1 Reference quinoline-amide tethered anticancer agents.

include inhibition of cellular promoting factors such as tubulin polymerization and topoisomerase.^{32,33} Recently, several research studies have described quinoline derivatives with anticancer efficacy *via* inhibition of kinases and inhibition of the anti-death Bcl-2 family of proteins^{34,35} (Fig. 1).

The amide pharmacophore is an important framework for developing drugs and discovery.³⁶ According to medicinal chemistry sources, one or more amide bonds serve as the basic component in more than 25% of natural and synthetic drugs available in the market.³⁷ The amide functional group enhances the anticancer activity by making molecules more polar as well as forming a hydrogen bond acceptor–donor domain with the target receptor.³⁸ Therefore, the introduction of an amide motif bearing a *cis*-vinyl group into the quinoline core is likely to significantly influence biological activity.³⁹

The aforementioned intriguing findings, combined with our ongoing quest for more potent anticancer agents, led to the molecular hybridization of the quinoline core and the bioactive triamide motif bearing a *cis*-vinyl group in order to integrate them into a single molecular framework and achieve a new hybrid that could have potential antiproliferative activity (Fig. 2). The study's goal is to look into the benefits of such hybridization in terms of predicted biological activity and to see whether this resulted in better biological activity for the produced hybrids. Lastly, we used *in vitro* tests to assess the antiproliferative action of the prepared quinoline-*cis*-vinyl triamide hybrids, as well as FACS and ELISA methods to determine the mechanism of cellular action.

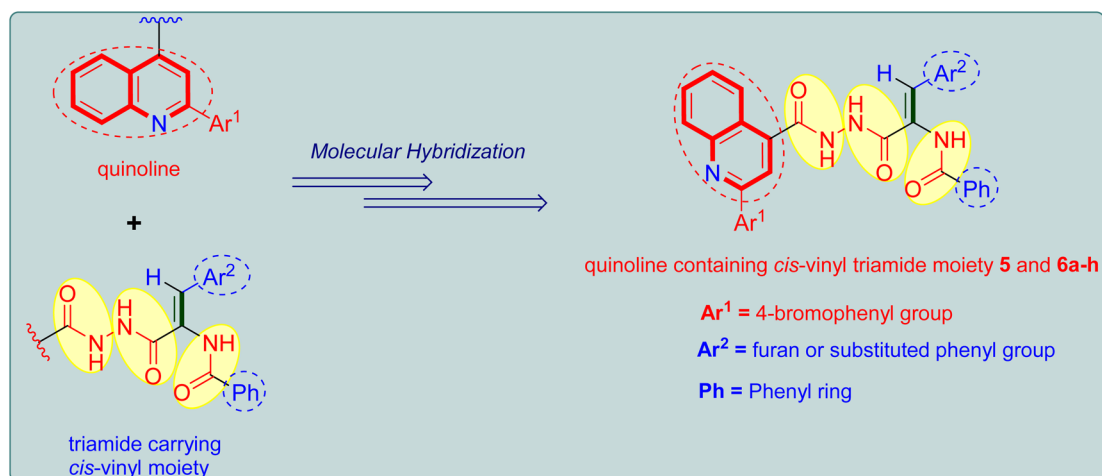


Fig. 2 Design strategy adopted for the design of target quinoline tethered *cis*-vinyl triamides **5** and **6a-h**.



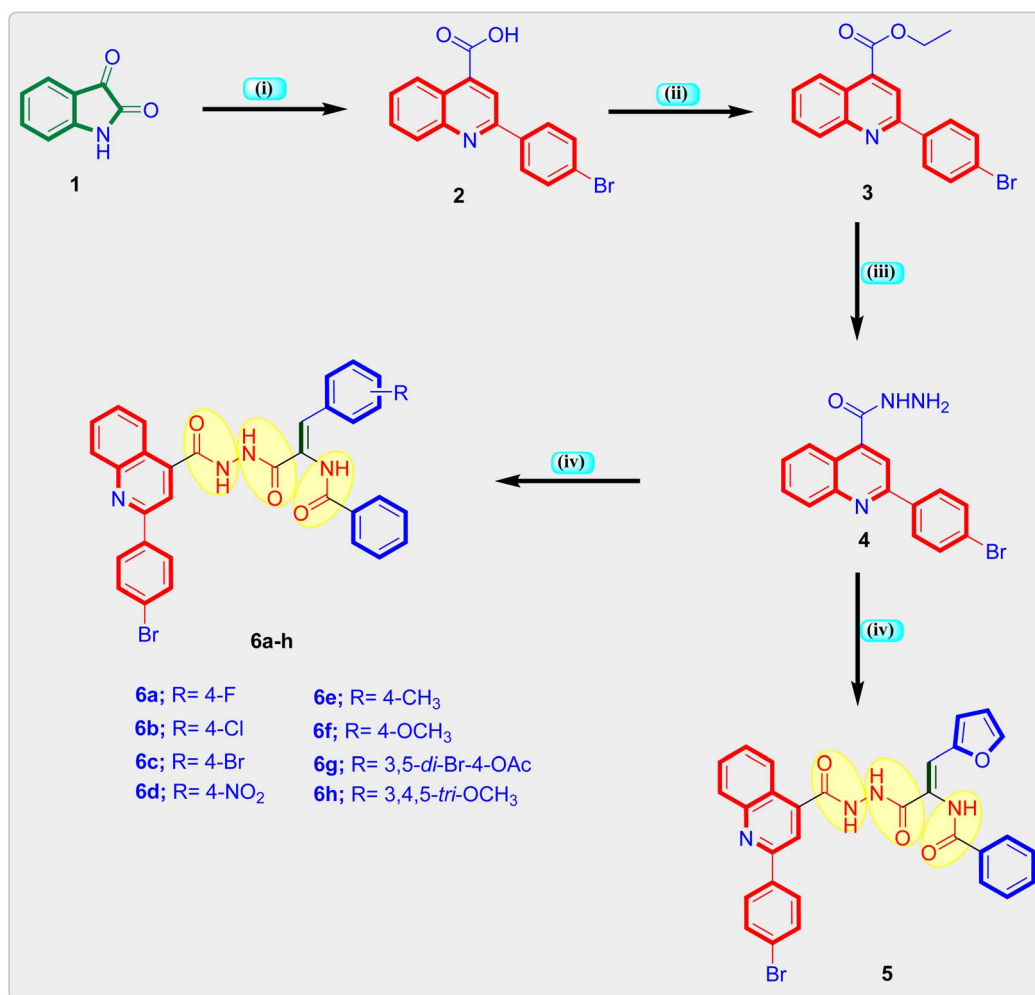
2. Results and discussion

2.1. Chemistry

The synthetic route used in the preparation of the intermediate and final quinoline based triamide compounds is depicted in Scheme 1. In the initial step appropriate 2-(4-bromoquinoline)-4-carboxylic acid **2** was obtained from reaction of isatin **1** and 4-bromoacetophenone in the presence of 33% KOH in pure ethanol by refluxing which was then heated to reflux in pure ethanol in the presence of concentrated sulphuric acid to obtain ethyl quinoline-4-carboxylate **3**.²⁶ This is followed by hydrazinolysis with pure hydrazine hydrate in boiling ethanol to furnish the key intermediate quinoline-4-carbohydrazide compound **4**.^{40,41} Lastly, final quinolone-linked triamide derivatives **5** and **6a-h** were obtained by the reaction of quinoline-4-carbohydrazide **4** and respective methyl 3-aryl-2-(benzamido)-2-propenoate derivative in freshly molten sodium acetate and glacial acetic acid by refluxing and yielding 64–78%. The formation of the quinoline linked triamide compounds **5** and **6a-h** in general were authenticated by ¹H-NMR, ¹³C-NMR and

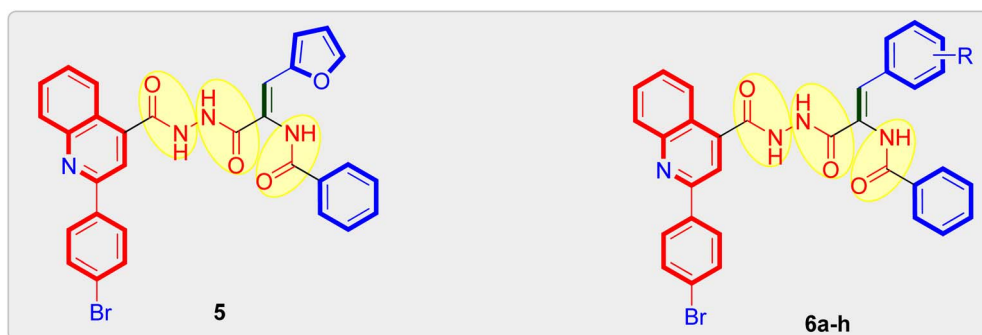
elemental analysis. ¹H-NMR spectra of the final quinoline-like triamide molecules displayed three broad singlets at range δ 10.89–9.99 ppm ascribed to the three amide protons and singlet peak at δ 7.48–7.37 ppm range assigned to olefinic (=CH) proton. The characteristic doublet signal at about δ 8.46–8.42 ppm is attributed to the C8-H of the quinoline motif. In addition, the protons of C7-H and C6-H of quinoline motif appeared as two triplet signals with one proton each in the range at δ 7.88–7.72 and 7.72–7.63 ppm, respectively.

The ¹³C-NMR spectra of the final compounds displayed signals for aromatic and olefinic carbon atoms were observed at around δ 153.09–107.71 ppm, whereas signals for aliphatic carbon atoms in compounds **6f**, **6e**, **6g** and **6h** were observed at around δ 60.54–20.65. The characteristic C2 carbon of quinoline moiety was identified in the range δ 155.03–155.00 ppm. Furthermore, the carbonyl carbons of the three amide functions were seen at about δ 168.85–164.45 ppm providing a substantial argument in support of the compounds' ascribed structures. Each of the target compounds was characterized using the melting point technique, and their purity was verified using the



Scheme 1 Global synthesis of quinoline-*cis*-vinyl triamide hybrids **5** and **6a-h**. Reagents: (i) 4-Br-C₆H₄COCH₃, 33% KOH, EtOH, reflux 24 h, yield = 89%; (ii) H₂SO₄, EtOH, reflux 12 h, yield = 80%; (iii) NH₂NH₂·H₂O, EtOH, reflux 4 h, yield = 77%; (iv) respective methyl 3-aryl-2-(benzamido)-2-propenoate, EtOH, reflux 20–22 h, yield: 64–78%.



Table 1 *In vitro* cytotoxic results (IC₅₀ values, μM) of quinoline tethered *cis*-vinyl triamides **5** and **6a–h** versus examined cell line

Comp. no.	R	IC ₅₀ (μM)	
		MCF-7	STU
5	—	6.60 ± 0.21	13.28 ± 0.43
6a	4-F	59.77 ± 1.93	13.28 ± 0.43
6b	4-Cl	8.29 ± 0.27	13.28 ± 0.43
6c	4-Br	19.25 ± 0.62	13.28 ± 0.43
6d	4-NO ₂	12.43 ± 0.40	13.28 ± 0.43
6e	4-CH ₃	3.03 ± 0.10	13.28 ± 0.43
6f	4-OCH ₃	1.87 ± 0.06	13.28 ± 0.43
6g	3,5-di-Br-4-OCOCH ₃	30.44 ± 0.98	13.28 ± 0.43
6h	3,4,5-tri-OCH ₃	15.63 ± 0.42	13.28 ± 0.43
STU	—	13.28 ± 0.43	13.28 ± 0.43

TLC method. The newly prepared quinoline-triamide molecules' analytical and spectral data (¹H-NMR and ¹³C-NMR spectra) agreed fully with the suggested structures.

2.2. Biology

2.2.1. Antiproliferative activity. The antiproliferative potential of the newly prepared quinoline tethered *cis*-vinyl triamide derivatives **5** and **6a–h** was assessed against the MCF-7 cell line in comparison to Staurosporin (STU) as reference standard drug. Based on obtained *in vitro* results, the majority of the quinoline tethered *cis*-vinyl triamide derivatives tested demonstrated moderate to significant antiproliferative action against the examined cancer cell line. Five compounds; **5**, **6b**, **6d**, **6e** and **6f** showed 1.06–7.10-fold more potent antiproliferative activity than the reference STU. Two compounds **6c** and **6h** showed antiproliferative activity with IC₅₀ values of 19.25 and 15.63 μM, respectively comparable to STU (IC₅₀ = 13.28 μM). The rest hybrids **6a** and **6g** showed modest antiproliferative activity with IC₅₀ of 59.77 and 30.44 μM, respectively. The antiproliferative activity correlation of quinoline tethered *cis*-vinyl triamide derivatives **5** and **6a–h** showed that among the quinoline-*cis* vinyl triamide derivatives, compounds bearing electron donating groups such as methyl; **6e** (IC₅₀ = 3.03 μM) and methoxy; **6f** (IC₅₀ = 1.87 μM) showed more potent antiproliferative activity than the other substituted derivatives with electron withdrawing groups and were found to be more potent than STU (IC₅₀ = 13.28 μM). Another interesting observation is that introducing three groups in the 3,4,5-position of

the phenyl ring attached to the *cis*-vinyl moiety, such as 3,5-dibromo-4-acetoxy group; **6g** (IC₅₀ = 30.44 μM) and 3,4,5-trimethoxy group; **6h** (IC₅₀ = 15.63 μM), resulted in low antiproliferative activity. It is also notable that replacement of substituted phenyl ring in *cis*-vinyl moiety with heterocyclic ring such as furan (IC₅₀ = 6.60 μM) resulted in increase in antiproliferative activity compared to reference drug STU. According to these findings, the examined quinoline tethered triamide motif bearing *cis*-vinyl group with furan function or *para*-substituted phenyl ring with electron donating group such as methyl or methoxy had a beneficial influence on antiproliferative activity Table 1.

2.2.2. Cell cycle analysis. The cell cycle is related to a series of events responsible for cell division and duplication.⁴² The cell cycle presents three distinct phases: G1, S and G2/M phase.⁴³ Due to the importance of the cell cycle in the process of tumor progression, we evaluated if the cell growth inhibition in MCF-7 occurred due to cell cycle arrest using FACS method. In the present study, flow cytometric measurement was utilized to investigate the effect of quinoline tethered [2-(4-methoxyphenyl)-*cis*-vinyl] triamide **6f** on cellular cycle progression in tested breast cancer cells. In the test, MCF-7 cells were treated with quinoline tethered [2-(4-methoxyphenyl)-*cis*-vinyl] triamide **6f** at a concentration of 1.87 μM, then incubated for 48 h. The cellular cycle distribution was analyzed to identify the definite phase at which quinoline tethered [2-(4-methoxyphenyl)-*cis*-vinyl] triamide **6f** can arrest the cell cycle. The results indicated that quinoline-[2-(4-methoxyphenyl)-*cis*-vinyl] triamide **6f**



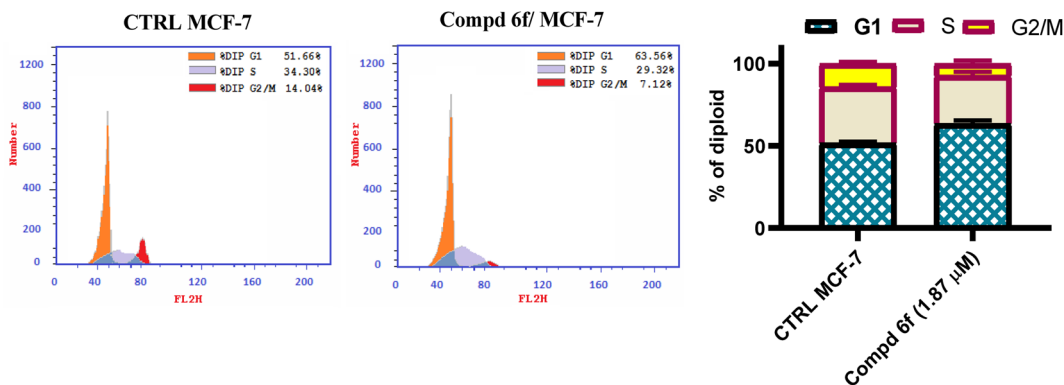


Fig. 3 Sample graph of quinoline-[2-(4-methoxyphenyl)-*cis*-vinyl] triamide **6f** treated MCF-7 cells compared to controls. This software calculates number of diploid cells in G1, S and G2/M phase of cellular cycle.

significantly declined the cellular population at G1 phase. It is observed that the percentage of cells at G1 phase was increased by 1.2-fold compared to controls (Fig. 3). Coordinately, the percentage of cells was decreased at S and G2/M phases from 34.30 and 14.04% in controls to 29.32 and 7.12%, respectively in compound **6f**-treated cells. These findings suggest that quinoline-[2-(4-methoxyphenyl)-*cis*-vinyl] triamide **6f** halted the cell cycle proliferation of the MCF-7 cells at G1 phase.

2.2.3. Apoptosis analysis. Apoptosis play an important role in organogenesis and in crafting complex tissues during embryonic growth, and in the preservation of tissue homeostasis in adult organism.⁴⁴ Numerous clinical disorders, including cancer, autoimmune illness and infectious diseases, are characterised by the deregulation of apoptosis.⁴⁵ To ensure the ability of quinoline tethered [2-(4-methoxyphenyl)-*cis*-vinyl] triamide **6f** to activate apoptosis, flow cytometric measurement was carried out using Annexin V which binds to phosphatidylserine declared on the outer layer of apoptotic cells and appears fluorescent green and PI which stains DNA and penetrates only dead cells. After 48 h of treatment with quinoline tethered [2-(4-methoxyphenyl)-*cis*-vinyl] triamide **6f** at the IC₅₀ concentration (1.87 μ M), the percentage of cells that are

survived was found to decrease. Additionally, there was a notable rise in the proportion of cells positive for Annexin V. It is notable that, the percentage of primary apoptotic cells was increased from 0.66% in DMSO controls to 9.52% in compound **6f**-treated cells. Meanwhile, the proportion of late apoptotic cells rose from 0.21% to 16.65% compared to DMSO controls (Fig. 4). These findings suggest that quinoline tethered [2-(4-methoxyphenyl)-*cis*-vinyl] triamide **6f** provoke apoptosis of MCF-7 cells.

2.2.4. Mitochondrial membrane potential. A major part of apoptosis process is played by mitochondria.⁴⁶ Several active proteins such as cytochrome C and factor that induces apoptosis are two of the active proteins found in mitochondria.⁴⁷ The release of such proteins after inhibition of mitochondrial membrane potential (MMP) is crucial in the propagation of apoptosis.⁴⁸ To confirm whether quinoline tethered [2-(4-methoxyphenyl)-*cis*-vinyl] triamide **6f** could lower the MMP of tested cancer cell line (MCF-7 cells), flow cytometry was used to track MMP following treatment of the examined cells with 1.87 μ M (IC₅₀ dose value) of compound **6f**. Results indicated that the tested cancer cells exhibited significant decrease in MMP. This decrease in MMP was linked to an

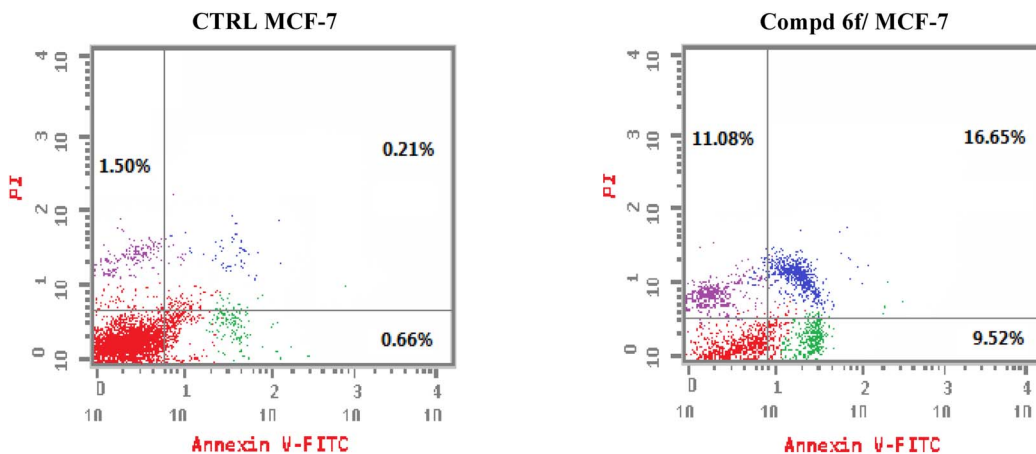


Fig. 4 Sample graph showing the impact on apoptotic ratio caused by quinoline-[2-(4-methoxyphenyl)-*cis*-vinyl] triamide **6f**-treated MCF-7 cells and compared to controls.

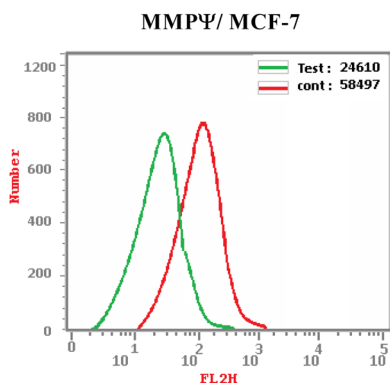


Fig. 5 Sample graph showing the effect on MMP caused by quinoline-[2-(4-methoxyphenyl)-*cis*-vinyl] triamide **6f**-treated MCF-7 cells and compared to controls.

increase in Annexin V positive cells. It is notable that, in comparison to DMSO controls, MCF-7 cells' MMP was 57.93% percent value lower (Fig. 5). According to this, quinoline tethered [2-(4-methoxyphenyl)-*cis*-vinyl] triamide **6f** cause MCF-7 cells to become dysfunction in their mitochondria, which in turn trigger apoptotic cellular death. These outcomes were consistent with early findings that EGFR-TK inhibitors promote apoptosis *via* the mitochondrial route.

2.2.5. EGFR tyrosine kinase inhibition analysis. EGFR have been implicated in a variety of cancer indications and other inappropriate mitogenic signalling disorders.⁴⁹ Clinical evidence demonstrates an association between EGFR over-expression and response to a number of anticancer therapeutics.⁵⁰ So EGFR and the activated downstream cascades represent a promising target for the establishment of therapeutic agents.⁵¹ As result of the effect of quinoline-[2-(4-methoxyphenyl)-*cis*-vinyl] triamide **6f** on the G1 phase of the cellular cycle where the protein synthesis required for the cell growth rises, the inhibition of EGFR tyrosine kinase was thought to be the expected mode of cellular action of this hybrid molecule. Thus, the purpose of this experiment was to assess the inhibitory activity of EGFR tyrosine kinase. The quinoline-[2-(4-methoxyphenyl)-*cis*-vinyl] triamide **6f** showed good activity

($IC_{50} = 0.19 \mu\text{M}$), which was comparable to that of Lapatinib ($IC_{50} = 0.17 \mu\text{M}$), a known potent EGFR inhibitor (Fig. 6). So it is concluded that quinoline-[2-(4-methoxyphenyl)-*cis*-vinyl] triamide **6f** exerted its antiproliferative activity through inhibition of EGFR tyrosine kinase.

3. Conclusions

A new set of quinoline-tethered *cis*-vinyl triamide hybrids **5** and **6a-h** was designed and constructed as inhibitors of EGFR tyrosine kinase for the treatment of breast cancer. All the prepared quinoline-tethered *cis*-vinyl triamide hybrids were screened for their *in vitro* antiproliferative activity and revealed moderate to potent activity. Among them, quinoline compounds **6e** bearing [2-(4-methylphenyl)-*cis*-vinyl] triamide and **6f** bearing [2-(4-methoxyphenyl)-*cis*-vinyl] triamide were found to be the most potent hybrids against the MCF-7 breast cancer cell line, with IC_{50} values of 1.87 and 1.88 μM , respectively, compared to STU ($IC_{50} = 13.77 \mu\text{M}$). Additional mechanistic studies demonstrated that quinoline-[2-(4-methoxyphenyl)-*cis*-vinyl] triamide **6f** effectively blocked the G1 phase of the cell cycle and was found to promote cellular apoptosis. It is notable that quinoline-[2-(4-methoxyphenyl)-*cis*-vinyl] triamide **6f** increased the percentage population at G1 phase by 1.2-fold more than controls. In addition, it boosted the level of both early and late apoptosis by almost 14.4- and 79.3-fold, respectively, compared to controls. Further mechanistic apoptotic studies confirmed that treatment in MCF-7 cells with the most active member; quinoline-[2-(4-methoxyphenyl)-*cis*-vinyl] triamide **6f**, decreased the level of MMP of MCF-7 cells (57.93% percent change value) less than controls. Notably, quinoline-[2-(4-methoxyphenyl)-*cis*-vinyl] triamide **6f** also demonstrated potent EGFR tyrosine kinase inhibition with an IC_{50} value of 0.19 μM , which was equipotent to reference standard Lapatinib ($IC_{50} = 0.17 \mu\text{M}$). The previous findings indicated that quinoline-[2-(4-methoxyphenyl)-*cis*-vinyl] triamide **6f** is a potent apoptosis-active anticancer molecule that exerted its action *via* EGFR tyrosine kinase inhibition as a promising structure that could serve as a novel template for developing powerful and selective agents in cancer therapy.

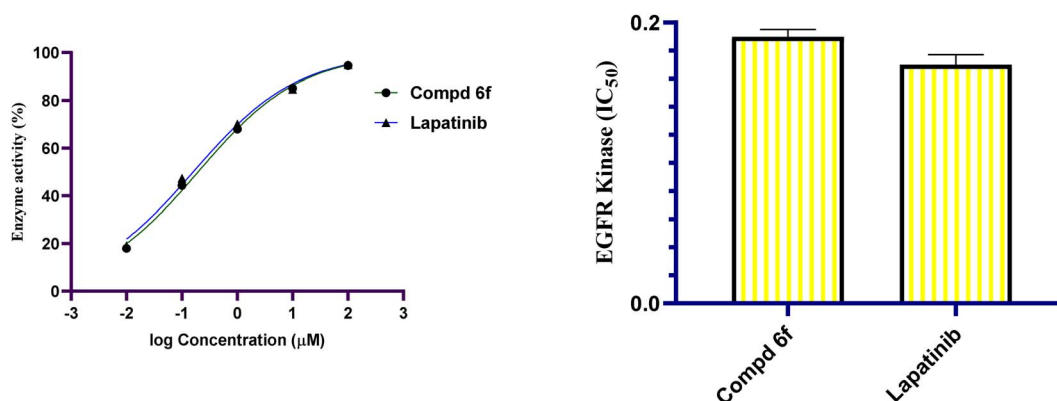


Fig. 6 Graphical illustration of the EGFR inhibitory activity (IC_{50} , μM) of quinoline-[2-(4-methoxyphenyl)-*cis*-vinyl] triamide **6f** treated compared to Lapatinib.



4. Experimental

4.1. Chemistry

4.1.1. General procedure for synthesis of (Z)-N-(1-aryl-3-(2-(4-bromophenyl)quinoline-4-carbonyl)hydrazinyl)-3-oxoprop-1-en-2-yl)benzamides 5 and 6a-h. An appropriate *cis*-methyl 3-aryl-2-(benzamido)-2-propenoate (1 mmol) was added to the mixture of quinoline-4-carbohydrazide **4** (0.342 g, 1 mmol) and anhydrous sodium acetate (0.098 g, 1.2 mmol) in glacial acetic acid (20 mL) and refluxed for 20–22 h. After consumption of quinoline-4-carbohydrazide compound **4** (checked by TLC), the reaction mixture was cooled to ambient room temperature and poured onto cold water. The precipitated solid was separated by filtration, washed with cold water (15 mL) and dried. The crude solid was chromatographed on silica gel using ethyl acetate/*n*-hexane as eluent to attain target quinoline tethered *cis*-vinyl triamide **5** and **6a-h**.

4.1.1.1 (Z)-N-(3-(2-(2-(4-Bromophenyl)quinoline-4-carbonyl)hydrazinyl)-1-(furan-2-yl)-3-oxoprop-1-en-2-yl)benzamide (5). Yield 76%; mp: 188–190 °C. ¹H-NMR (400 MHz, DMSO-*d*₆) δ: 10.80 (s, 1H, NH), 10.49 (s, 1H, NH), 9.99 (s, 1H, NH), 8.42 (d, *J* = 8.4 Hz, 1H, C8-H quinoline), 8.26 (d, *J* = 8.3 Hz, 2H), 8.19–8.14 (m, 2H), 8.13–8.07 (m, 2H), 7.88 (t, *J* = 7.6 Hz, C7-H quinoline), 7.84–7.78 (m, 3H), 7.71 (t, *J* = 7.7 Hz, 2H, C6-H quinoline and Ar-H), 7.63 (dd, *J* = 8.3, 6.2 Hz, 1H), 7.56 (t, *J* = 7.5 Hz, 2H), 7.35 (s, 1H), 6.82 (d, *J* = 3.5 Hz, 1H), 6.63 (dd, *J* = 3.5, 1.8 Hz, 1H). ¹³C-NMR (101 MHz, DMSO) δ 166.32, 166.11, 164.45, 155.01, 150.03, 148.30, 145.42, 141.99, 137.75, 134.30, 132.45, 132.14, 131.06, 129.97, 129.74, 128.75, 128.47, 127.98, 126.18, 126.01, 124.22, 124.05, 119.42, 117.14, 115.14, 112.88. C₃₀H₂₁BrN₄O₄ (581.42): calcd: C, 61.97; H, 3.64; N, 9.64. Found: C, 62.09; H, 3.78; N, 9.51.

4.1.1.2. (Z)-N-(3-(2-(2-(4-Bromophenyl)quinoline-4-carbonyl)hydrazinyl)-1-(4-fluorophenyl)-3-oxoprop-1-en-2-yl)benzamide (6a). Yield 68%; mp: 177–179 °C. ¹H-NMR (400 MHz, DMSO-*d*₆) δ 10.68 (d, *J* = 90.2 Hz, 2H, 2NH), 10.11 (s, 1H, NH), 8.46 (d, *J* = 8.4 Hz, 1H, C8-H quinoline), 8.31–8.23 (m, 2H, Ar-H), 8.16 (t, *J* = 4.3 Hz, 2H, Ar-H), 8.06 (d, *J* = 7.6 Hz, 2H, Ar-H), 7.87 (t, *J* = 7.6 Hz, 1H, C7-H quinoline), 7.83–7.77 (m, 2H, Ar-H), 7.71 (td, *J* = 5.6, 2.9 Hz, 3H, C6-H quinoline and Ar-H), 7.65–7.59 (m, 1H, Ar-H), 7.55 (t, *J* = 7.4 Hz, 2H, Ar-H), 7.43 (s, 1H, =CH), 7.26 (td, *J* = 8.9, 1.6 Hz, 2H, Ar-H). ¹³C-NMR (101 MHz, DMSO) δ 168.85, 166.50, 166.05, 156.50, 155.00, 148.32, 142.34, 142.19, 137.80, 134.03, 132.45, 132.25, 132.21, 132.13, 131.06, 131.00, 129.96, 129.74, 128.79, 128.47, 127.91, 126.12, 124.22, 117.14, 116.19, 115.98. C₃₂H₂₂BrFN₄O₃ (609.44): calcd: C, 63.06; H, 3.64; N, 9.19. Found: C, 62.95; H, 3.55; N, 9.33.

4.1.1.3. (Z)-N-(3-(2-(2-(4-Bromophenyl)quinoline-4-carbonyl)hydrazinyl)-1-(4-chlorophenyl)-3-oxoprop-1-en-2-yl)benzamide (6b). Yield 73%; mp: 185–187 °C. ¹H-NMR (400 MHz, DMSO-*d*₆) δ 10.83 (s, 1H, NH), 10.58 (s, 1H, NH), 10.13 (s, 1H, NH), 8.43 (d, *J* = 8.4 Hz, 1H, C8-H quinoline), 8.27 (d, *J* = 8.2 Hz, 2H, Ar-H), 8.16 (s, 2H, Ar-H), 8.08–8.02 (m, 2H, Ar-H), 7.88 (t, *J* = 7.6 Hz, 1H, C7-H quinoline), 7.81 (d, *J* = 8.2 Hz, 2H, Ar-H), 7.72 (t, *J* = 7.7 Hz, 2H, C6-H quinoline), 7.67 (d, *J* = 8.3 Hz, 2H, Ar-H), 7.62 (d, *J* = 7.2 Hz, 1H, Ar-H), 7.55 (t, *J* = 7.5 Hz, 2H, Ar-H), 7.48 (d, *J* = 8.3 Hz, 2H, Ar-H), 7.40 (s, 1H, =CH). ¹³C-NMR (101 MHz,

DMSO) δ 166.49, 166.15, 164.96, 155.02, 148.30, 141.98, 137.74, 133.95, 133.84, 133.43, 132.46, 132.29, 131.61, 131.07, 129.98, 129.80, 129.75, 129.53, 129.13, 128.79, 128.48, 128.00, 125.98, 124.23, 124.05, 117.15. C₃₂H₂₂BrClN₄O₃ (625.90): calcd: C, 61.41; H, 3.54; N, 8.95. Found: C, 61.59; H, 3.39; N, 9.09.

4.1.1.4. (Z)-N-(1-(4-Bromophenyl)-3-(2-(2-(4-bromophenyl)quinoline-4-carbonyl)hydrazinyl)-3-oxoprop-1-en-2-yl)benzamide (6c). Yield 78%; mp: 191–193 °C. ¹H-NMR (400 MHz, DMSO-*d*₆) δ 10.83 (s, 1H, NH), 10.58 (s, 1H, NH), 10.13 (s, 1H, NH), 8.43 (d, *J* = 8.4 Hz, 1H, C8-H quinoline), 8.26 (d, *J* = 8.2 Hz, 2H, Ar-H), 8.17 (d, *J* = 7.7 Hz, 2H, Ar-H), 8.05 (d, *J* = 7.7 Hz, 2H, Ar-H), 7.87 (t, *J* = 7.8 Hz, 1H, C7-H quinoline), 7.80 (d, *J* = 8.1 Hz, 2H, Ar-H), 7.71 (t, *J* = 7.7 Hz, 2H, C6-H quinoline), 7.60 (h, *J* = 8.0, 7.3 Hz, 6H, Ar-H), 7.37 (s, 1H, =CH). ¹³C-NMR (101 MHz, DMSO) δ 166.46, 166.14, 164.95, 155.02, 148.31, 141.99, 137.75, 133.96, 133.80, 132.46, 132.29, 132.05, 131.84, 131.07, 129.99, 129.91, 129.75, 129.55, 128.79, 128.49, 127.99, 126.00, 124.23, 124.06, 122.59, 117.15. C₃₂H₂₂Br₂N₄O₃ (670.35): calcd: C, 57.33; H, 3.31; N, 8.36. Found: C, 57.42; H, 3.36; N, 8.29.

4.1.1.5. (Z)-N-(3-(2-(2-(4-Bromophenyl)quinoline-4-carbonyl)hydrazinyl)-1-(4-nitrophenyl)-3-oxoprop-1-en-2-yl)benzamide (6d). Yield 69%; mp: 207–209 °C. ¹H-NMR (400 MHz, DMSO-*d*₆) δ 10.89 (s, 1H, NH), 10.72 (s, 1H, NH), 10.30 (s, 1H, NH), 8.44 (d, *J* = 8.3 Hz, 1H, C8-H quinoline), 8.27 (dt, *J* = 9.0, 2.9 Hz, 4H, Ar-H), 8.18 (t, *J* = 4.2 Hz, 2H, Ar-H), 8.05 (d, *J* = 7.7 Hz, 2H, Ar-H), 7.90 (d, *J* = 8.7 Hz, 3H, Ar-H), 7.81 (d, *J* = 8.1 Hz, 2H, Ar-H), 7.72 (t, *J* = 7.7 Hz, 1H, C7-H quinoline), 7.63 (t, *J* = 7.4 Hz, 1H, C6-H quinoline), 7.56 (t, *J* = 7.5 Hz, 2H, Ar-H), 7.43 (s, 1H, =CH). ¹³C-NMR (101 MHz, DMSO) δ 166.53, 166.14, 164.73, 155.03, 148.31, 147.25, 142.33, 141.88, 141.54, 137.74, 132.45, 132.37, 131.07, 130.83, 129.99, 129.76, 128.82, 128.55, 128.01, 127.79, 127.62, 125.96, 125.90, 124.17, 124.05, 117.18. C₃₂H₂₂BrN₅O₅ (636.45): calcd: C, 60.39; H, 3.48; N, 11.00. Found: C, 60.24; H, 3.57; N, 11.12.

4.1.1.6. (Z)-N-(3-(2-(2-(4-Bromophenyl)quinoline-4-carbonyl)hydrazinyl)-3-oxo-1-*p*-tolylprop-1-en-2-yl)benzamide (6e). Yield 70%; mp: 211–213 °C. ¹H-NMR (400 MHz, DMSO-*d*₆) δ 10.79 (s, 1H, NH), 10.49 (s, 1H, NH), 10.07 (s, 1H, NH), 8.44 (d, *J* = 8.4 Hz, 1H, C8-H quinoline), 8.27 (d, *J* = 8.3 Hz, 2H, Ar-H), 8.17 (d, *J* = 9.0 Hz, 2H, Ar-H), 8.07 (d, *J* = 7.6 Hz, 2H, Ar-H), 7.88 (t, *J* = 7.5 Hz, 1H, C7-H quinoline), 7.81 (d, *J* = 8.2 Hz, 2H, Ar-H), 7.72 (t, *J* = 7.8 Hz, 1H, C6-H quinoline), 7.58 (dt, *J* = 15.1, 7.2 Hz, 5H, Ar-H), 7.42 (s, 1H, =CH), 7.22 (d, *J* = 7.9 Hz, 2H, Ar-H), 2.32 (s, 3H, Ar-CH₃). ¹³C-NMR (101 MHz, DMSO) δ 167.67, 166.78, 166.10, 164.42, 155.03, 148.30, 145.77, 141.91, 137.74, 135.63, 133.91, 133.45, 132.42, 131.43, 131.08, 130.00, 129.75, 128.82, 128.38, 128.02, 127.40, 125.96, 124.24, 124.04, 117.64, 117.15, 20.65. C₃₃H₂₅BrN₄O₃ (605.48): calcd: C, 65.46; H, 4.16; N, 9.25. Found: C, 65.60; H, 4.28; N, 9.11.

4.1.1.7. (Z)-N-(3-(2-(2-(4-Bromophenyl)quinoline-4-carbonyl)hydrazinyl)-1-(4-methoxyphenyl)-3-oxoprop-1-en-2-yl)benzamide (6f). Yield 75%; mp: 206–208 °C. ¹H-NMR (400 MHz, DMSO-*d*₆) δ 10.76 (s, 1H, NH), 10.43 (s, 1H, NH), 10.04 (s, 1H, NH), 8.44 (d, *J* = 8.4 Hz, 1H, C8-H quinoline), 8.30–8.23 (m, 2H, Ar-H), 8.19–8.13 (m, 2H, Ar-H), 8.12–8.05 (m, 2H, Ar-H), 7.87 (t, *J* = 7.5 Hz, 1H, C7-H quinoline), 7.84–7.77 (m, 2H, Ar-H), 7.71 (t, *J* = 7.8 Hz, 1H, C6-H quinoline), 7.63 (d, *J* = 8.5 Hz, 3H, Ar-H), 7.55



(t, $J = 7.4$ Hz, 2H, Ar-H), 7.43 (s, 1H, =CH), 6.98 (d, $J = 8.8$ Hz, 2H, Ar-H), 3.78 (s, 3H, Ar-OCH₃). ¹³C-NMR (101 MHz, DMSO) δ 166.44, 166.16, 165.27, 160.36, 155.01, 142.10, 140.27, 137.76, 134.18, 132.46, 132.17, 131.83, 131.42, 130.83, 129.97, 129.74, 128.77, 128.46, 127.97, 126.85, 126.75, 126.04, 124.22, 124.07, 117.13, 114.60, 55.72. C₃₃H₂₅BrN₄O₄ (621.48): calcd; C, 63.78; H, 4.05; N, 9.02. Found: C, 63.86; H, 3.96; N, 8.95.

4.1.1.8. (*Z*)-4-(2-Benzamido-3-(2-(2-(4-bromophenyl)quinoline-4-carbonyl)hydrazinyl)-3-oxoprop-1-enyl)-2,6-dibromophenyl acetate (**6g**). Yield 64%; mp: 181–183 °C. ¹H-NMR (400 MHz, DMSO-*d*₆) δ 10.86 (s, 1H, NH), 10.65 (s, 1H, NH), 10.22 (s, 1H, NH), 8.43 (d, $J = 8.5$ Hz, 1H, C8-H quinoline), 8.27 (d, $J = 8.4$ Hz, 2H, Ar-H), 8.17 (d, $J = 8.8$ Hz, 2H, Ar-H), 8.03 (d, $J = 10.7$ Hz, 4H, Ar-H), 7.88 (t, $J = 7.6$ Hz, C7-H quinoline), 7.81 (d, $J = 8.3$ Hz, 2H, Ar-H), 7.71 (t, $J = 7.8$ Hz, 1H, C6-H quinoline), 7.63 (t, $J = 7.2$ Hz, 1H, Ar-H), 7.56 (t, $J = 7.5$ Hz, 2H, Ar-H), 7.40 (s, 1H, =CH), 2.40 (s, 3H, Ar-OCOCH₃). ¹³C-NMR (101 MHz, DMSO) δ 166.48, 166.18, 165.19, 165.17, 155.02, 148.31, 142.06, 139.30, 137.76, 134.15, 132.47, 132.20, 131.61, 131.39, 131.08, 130.04, 129.75, 129.69, 128.77, 128.45, 128.23, 128.00, 126.05, 126.01, 124.24, 124.07, 117.13, 21.41. C₃₄H₂₃Br₂N₄O₅ (807.28): calcd; C, 50.59; H, 2.87; N, 6.94. Found: C, 50.44; H, 2.79; N, 7.07.

4.1.1.9. (*Z*)-*N*-(3-(2-(2-(4-Bromophenyl)quinoline-4-carbonyl)hydrazinyl)-3-oxo-1-(3,4,5-trimethoxyphenyl)prop-1-en-2-yl)benzamide (**6h**). Yield 67%; mp: 169–171 °C. ¹H-NMR (400 MHz, DMSO-*d*₆) δ 10.80 (s, 1H, NH), 10.51 (s, 1H, NH), 10.10 (s, 1H, NH), 8.45 (dd, $J = 8.4, 1.4$ Hz, 1H, C8-H quinoline), 8.31–8.23 (m, 2H, Ar-H), 8.17 (d, $J = 10.0$ Hz, 2H, Ar-H), 8.12 (dd, $J = 7.1, 2.0$ Hz, 2H, Ar-H), 7.88 (t, $J = 7.5$ Hz, C7-H quinoline), 7.84–7.78 (m, 2H, Ar-H), 7.72 (t, $J = 7.7$ Hz, 1H, C6-H quinoline), 7.62 (t, $J = 7.4$ Hz, 1H, Ar-H), 7.55 (t, $J = 7.5$ Hz, 2H, Ar-H), 7.48 (s, 1H, =CH), 7.03 (s, 2H, Ar-H), 3.68 (s, 3H, OCH₃), 3.63 (s, 6H, 2OCH₃). ¹³C-NMR (101 MHz, DMSO) δ 166.48, 166.13, 164.95, 155.02, 153.09, 152.91, 148.31, 142.04, 138.72, 137.76, 134.00, 132.46, 132.28, 131.90, 131.07, 129.98, 129.74, 128.71, 128.40, 128.14, 127.97, 126.03, 124.23, 124.07, 117.13, 107.71, 60.54, 56.08. C₃₅H₂₉BrN₄O₆ (681.53): calcd; C, 61.68; H, 4.29; N, 8.22. Found: C, 61.81; H, 4.36; N, 8.10.

4.2. Biological studies

All the experimental procedure used in the biological studies were shown in the ESI.†

Data availability

The authors confirm that the data supporting the findings of this study are available within the article and/or its ESI.†

Conflicts of interest

No potential conflict of interest was reported by the author(s).

Acknowledgements

This work was supported by the Deanship of Scientific Research, Vice Presidency for Graduate Studies and Scientific

Research, King Faisal University, Saudi Arabia (Grant No. KFU241438). The authors extend their appreciation to Princess Nourah Bint Abdulrahman University Researchers Supporting Project number (PNURSP2024R465), Princess Nourah Bint Abdulrahman University, Riyadh, Saudi Arabia, and the authors extend their appreciation to the Deanship of Scientific Research and Graduate Studies at King Khalid University for funding this work through the Large Research Project under grant number RGP2/61/45.

References

- 1 C. Santucci, S. Mignozzi, M. Malvezzi, P. Boffetta, G. Collatuzzo, F. Levi, C. La Vecchia and E. Negri, European cancer mortality predictions for the year 2024 with focus on colorectal cancer, *Ann. Oncol.*, 2024, **35**, 308–316.
- 2 R. L. Siegel, A. N. Giaquinto and A. Jemal, Cancer statistics, *Ca-Cancer J. Clin.*, 2024, **74**, 12–49.
- 3 P. Nenclares and K. J. Harrington, The biology of cancer, *Medicine*, 2020, **48**, 67–72.
- 4 K. M. Cuthrell and N. Tzenios, Breast Cancer: Updated and Deep Insights, *Int. Res. J. Oncol.*, 2023, **6**, 104–118.
- 5 M. Ensenyat-Mendez, P. Llinàs-Arias, J. I. J. Orozco, S. Íñiguez-Muñoz, M. P. Salomon, B. Sesé, M. L. DiNome and D. M. Marzese, Current Triple-Negative Breast Cancer Subtypes: Dissecting the Most Aggressive Form of Breast Cancer, *Front. Oncol.*, 2021, **11**, 681476–681483.
- 6 J. Wang and S.-G. Wu, Breast Cancer: An Overview of Current Therapeutic Strategies, Challenge, and Perspectives, *Breast Cancer: Targets Ther.*, 2023, **15**, 721–730.
- 7 J. G. Elmore and C. I. Lee, Toward More Equitable Breast Cancer Outcomes, *JAMA*, 2024, **331**, 1896–1897.
- 8 Brianna and S. H. Lee, Chemotherapy: how to reduce its adverse effects while maintaining the potency?, *Med. Oncol.*, 2023, **40**, 88.
- 9 M. Puzzo, M. De Santo, C. Morelli, A. Leggio and L. Pasqua, The Advent of Molecular Targeted Therapies Against Cancer. Toward Multi-Targeting Drugs Through Materials Engineering: A Possible Future Scenario, *Small Sci.*, 2024, 2400113.
- 10 H. Jin, L. Wang and R. Bernards, Rational combinations of targeted cancer therapies: background, advances and challenges, *Nat. Rev. Drug Discovery*, 2023, **22**, 213–234.
- 11 M. L. Uribe, I. Marrocco and Y. Yarden, EGFR in Cancer: Signaling Mechanisms, Drugs, and Acquired Resistance, *Cancers*, 2021, **13**, 2748.
- 12 A. W. Burgess, Regulation of Signaling from the Epidermal Growth Factor Family, *J. Phys. Chem. B*, 2022, **126**, 7475–7485.
- 13 A. Dang, S. Dang and B. Vallish, Efficacy and Safety of EGFR Inhibitors in the Treatment of EGFRPositive NSCLC Patients: A Meta-analysis, *Rev. Recent Clin. Trials*, 2021, **16**, 193–201.
- 14 S.-Y. Liu, S.-Y. M. Liu, W.-Z. Zhong and Y.-L. Wu, Targeted Therapy in Early Stage Non-small Cell Lung Cancer, *Curr. Treat. Options Oncol.*, 2022, **23**, 1169–1184.



- 15 S. Halder, S. Basu, S. P. Lall, A. K. Ganti, S. K. Batra and P. Seshacharyulu, Targeting the EGFR signaling pathway in cancer therapy: What's new in 2023?, *Expert Opin. Ther. Targets*, 2023, **27**, 305–324.
- 16 K. S. Alharbi, M. A. Javed Shaikh, O. Afzal, A. S. Alfawaz Altamimi, W. H. Almalki, S. I. Alzarea, I. Kazmi, F. A. Al-Abbasi, S. K. Singh, K. Dua and G. Gupta, An overview of epithelial growth factor receptor (EGFR) inhibitors in cancer therapy, *Chem. Biol. Interact.*, 2022, **366**, 110108.
- 17 F. Volta, S. La Monica, A. Leonetti, L. Gnetti, M. Bonelli, A. Cavazzoni, C. Fumarola, M. Galetti, K. Eltayeb, R. Minari, P. G. Petronini, M. Tiseo and R. Alfieri, Intrinsic Resistance to Osimertinib in EGFR Mutated NSCLC Cell Lines Induced by Alteration in Cell-Cycle Regulators, *Targeted Oncol.*, 2023, **18**, 953–964.
- 18 D. Nasser Binjawhar, F. A. Al-Salmi, M. A. Alghamdi, A. s. Alqahtani, E. Fayad, R. M. Saleem, I. Zaki and A. M. Youssef Moustafa, Design, Synthesis, and Biological Evaluation of Newly Synthesized Cinnamide-Fluorinated Containing Compounds as Bioactive Anticancer Agents, *ACS Omega*, 2024, **9**, 18505–18515.
- 19 R. Roskoski, Properties of FDA-approved small molecule protein kinase inhibitors: A 2024 update, *Pharmacol. Res.*, 2024, **200**, 107059.
- 20 N. Ryad, A. A. Elmaaty, I. M Ibrahim, A. H. Ahmed Maghrabi, M. A. Yahya Alahdal, R. M. Saleem, I. Zaki and L. M. A. A. Ghany, Harnessing molecular hybridization approach to discover novel quinoline EGFR-TK inhibitors for cancer treatment, *Future Med. Chem.*, 2024, **16**, 1087–1107.
- 21 V. Yadav, J. Reang, V. Sharma, J. Majeed, P. C. Sharma, K. Sharma, N. Giri, A. Kumar and R. K. Tonk, Quinoline-derivatives as privileged scaffolds for medicinal and pharmaceutical chemists: A comprehensive review, *Chem. Biol. Drug Des.*, 2022, **100**, 389–418.
- 22 O. O. Ajani, K. T. Iyaye and O. T. Ademosun, Recent advances in chemistry and therapeutic potential of functionalized quinoline motifs—a review, *RSC Adv.*, 2022, **12**, 18594–18614.
- 23 D. N. Binjawhar, F. A. Al-Salmi, O. A. A. Ali, M. A. Alghamdi, E. Fayad, R. M. Saleem, I. Zaki and N. Farouk, Design, synthesis and cytotoxic activity of molecular hybrids based on quinolin-8-yloxy and cinnamide hybrids and their apoptosis inducing property, *RSC Adv.*, 2024, **14**, 11443–11451.
- 24 C. dos Santos Chagas, F. L. A. Fonseca and I. A. Bagatin, Quinoline-derivative coordination compounds as potential applications to antibacterial and antineoplastic drugs, *Mater. Sci. Eng. C*, 2019, **98**, 1043–1052.
- 25 M. Mohasin, M. Zafer Alam, Q. Ullah, A. Ahmad, P. F. Rahaman and S. A. Khan, A Review on Synthesis and Biological Applications of Quinoline Derivative as Fused Aromatic Compounds, *Polycyclic Aromat. Compd.*, 2024, 1–30.
- 26 M. Ilakiyalakshmi and A. Arumugam Napoleon, Review on recent development of quinoline for anticancer activities, *Arabian J. Chem.*, 2022, **15**, 104168.
- 27 S. Hu, J. Chen, J.-X. Cao, S.-S. Zhang, S.-X. Gu and F.-E. Chen, Quinolines and isoquinolines as HIV-1 inhibitors: Chemical structures, action targets, and biological activities, *Bioorg. Chem.*, 2023, **136**, 106549.
- 28 H. M. Abd El-Lateef, A. A. Elmaaty, L. M. A. Abdel Ghany, M. S. Abdel-Aziz, I. Zaki and N. Ryad, Design and Synthesis of 2-(4-Bromophenyl)Quinoline-4-Carbohydrazide Derivatives via Molecular Hybridization as Novel Microbial DNA-Gyrase Inhibitors, *ACS Omega*, 2023, **8**, 17948–17965.
- 29 I. A. Bala, O. F. Al Sharif, A. M. Asiri and R. M. El-Shishtawy, Quinoline: A versatile bioactive scaffold and its molecular hybridization, *Results Chem.*, 2024, **7**, 101529.
- 30 V. Snehi, H. Verma, S. Saha, S. Kumar and D. Pathak, An extensive review on biological interest of quinoline and its analogues, *Int. J. Sci. Healthcare Res.*, 2023, **8**, 45–66.
- 31 Y. Chauhan, K. Neha, S. Wakode, M. Shahfaiz, R. B. Bodla and K. Sharma, Progression and Expansion of Quinoline as Bioactive Moiety: A Patent Review, *Pharm. Pat. Anal.*, 2023, **12**, 287–314.
- 32 Y. Ren, Y. Ruan, B. Cheng, L. Li, J. Liu, Y. Fang and J. Chen, Design, synthesis and biological evaluation of novel acridine and quinoline derivatives as tubulin polymerization inhibitors with anticancer activities, *Bioorg. Med. Chem.*, 2021, **46**, 116376.
- 33 H. K. Swedan, A. E. Kassab, E. M. Gedawy and S. E. Elmeligie, Topoisomerase II inhibitors design: Early studies and new perspectives, *Bioorg. Chem.*, 2023, **136**, 106548.
- 34 T. Fan, Y. Ji, D. Chen, X. Peng, J. Ai and B. Xiong, Design, synthesis and biological evaluation of 4-aminoquinoline derivatives as receptor-interacting protein kinase 2 (RIPK2) inhibitors, *J. Enzyme Inhib. Med. Chem.*, 2023, **38**, 282–293.
- 35 R. Hamdy, S. A. Elseginy, N. I. Ziedan, A. T. Jones and A. D. Westwell, New Quinoline-Based Heterocycles as Anticancer Agents Targeting Bcl-2, *Molecules*, 2019, **24**, 1274.
- 36 H. M. Abd El-Lateef, E. E. M. Toson, A. H. Abu Almaaty, R. M. Saleem, A. H. A. Maghrabi, E. H. El-Sayed, I. Zaki and M. M. Youssef, Synthesis, Characterization and Biological Evaluation of New Enamide Fluorinated-Schiff Base Derivatives as Potential Cytotoxic and Apoptosis-Inducing Agents, *ChemistrySelect*, 2023, **8**, e202303070.
- 37 C. Zhao, Y. Wang, Q. Pham, C. Dai, A. Chatterjee and M. Wasa, Chemical Tagging of Bioactive Amides by Cooperative Catalysis: Applications in the Syntheses of Drug Conjugates, *J. Am. Chem. Soc.*, 2023, **145**, 14233–14250.
- 38 Z. S. El-Fakharany, Y. M. Nissan, N. K. Sedky, R. K. Arafa and S. M. Abou-Seri, New proapoptotic chemotherapeutic agents based on the quinolone-3-carboxamide scaffold acting by VEGFR-2 inhibition, *Sci. Rep.*, 2023, **13**, 11346.
- 39 K. O. Mohamed, I. Zaki, I. M. El-Deen and M. K. Abdelhameid, A new class of diamide scaffold: Design, synthesis and biological evaluation as potent antimetabolic agents, tubulin polymerization inhibition and apoptosis inducing activity studies, *Bioorg. Chem.*, 2019, **84**, 399–409.
- 40 H. M. Abd El-Lateef, L. M. A. Ghany, R. M. Saleem, A. H. A. Maghrabi, M. A. Y. Alahdal, E. H. K. Ali, B. Y. Beshay, I. Zaki and R. E. Masoud, Design, synthesis



- and antiproliferative screening of newly synthesized coumarin-acrylamide hybrids as potential cytotoxic and apoptosis inducing agents, *RSC Adv.*, 2023, **13**, 32547–32557.
- 41 L. M. A. A. Ghany, N. Ryad, M. S. Abdel-Aziz, H. M. A. El-Lateef, I. Zaki and B. Y. Beshay, Design, synthesis, antimicrobial evaluation, and molecular modeling of new sulfamethoxazole and trimethoprim analogs as potential DHPS/DHFR inhibitors, *J. Mol. Struct.*, 2024, **1309**, 138170–138183.
- 42 K. Gousias, T. Theocharous and M. Simon, Mechanisms of Cell Cycle Arrest and Apoptosis in Glioblastoma, *Biomed*, 2022, **10**, 564.
- 43 X. Guo and L. Chen, From G1 to M: a comparative study of methods for identifying cell cycle phases, *Briefings Bioinf.*, 2024, **25**, 517–526.
- 44 D. Bertheloot, E. Latz and B. S. Franklin, Necroptosis, pyroptosis and apoptosis: an intricate game of cell death, *Cell. Mol. Immunol.*, 2021, **18**, 1106–1121.
- 45 E. Ozyerli-Goknar and T. Bagci-Onder, Epigenetic Deregulation of Apoptosis in Cancers, *Cancers*, 2021, **13**, 3210.
- 46 S. Dadsena, C. Zollo and A. J. García-Sáez, Mechanisms of mitochondrial cell death, *Biochem. Soc. Trans.*, 2021, **49**, 663–674.
- 47 M. Abate, A. Festa, M. Falco, A. Lombardi, A. Luce, A. Grimaldi, S. Zappavigna, P. Sperlongano, C. Irace, M. Caraglia and G. Misso, Mitochondria as playmakers of apoptosis, autophagy and senescence, *Semin. Cell Dev. Biol.*, 2020, **98**, 139–153.
- 48 K. Takács-Vellai, Apoptosis and Autophagy, Different Modes of Cell Death: How to Utilize Them to Fight Diseases?, *Int. J. Mol. Sci.*, 2023, **24**, 11609.
- 49 H. Liu, B. Zhang and Z. Sun, Spectrum of EGFR aberrations and potential clinical implications: insights from integrative pan-cancer analysis, *Cancer Commun.*, 2020, **40**, 43–59.
- 50 E. N. Alsaifi, S. Thavaraj, N. Sarvestani, O. Novoplansky, M. Elkabets, B. Ayaz, M. Tavassoli and M. F. Legends, EGFR overexpression increases radiotherapy response in HPV-positive head and neck cancer through inhibition of DNA damage repair and HPV E6 downregulation, *Cancer Lett.*, 2021, **498**, 80–97.
- 51 A. E. Maennling, M. K. Tur, M. Niebert, T. Klockenbring, F. Zeppernick, S. Gattenlöhner, I. Meinhold-Heerlein and A. F. Hussain, Molecular Targeting Therapy against EGFR Family in Breast Cancer: Progress and Future Potentials, *Cancers*, 2019, **11**, 1826.

